

## Surface Area of Oil Shale and its Solid Pyrolysis Products Depending on the Particle Size

Heliis Pikkor, Birgit Maaten, Zachariah Steven Baird, Oliver Järvik, Alar Konist, Heidi Lees\*

Department of Energy Technology, Tallinn University of Technology, Ehitajate tee 5, Tallinn, 19086, Estonia  
[heidi.lees@taltech.ee](mailto:heidi.lees@taltech.ee)

Oil shale is currently used for electricity and oil production. The production of the latter produces large quantities of residue, i.e. semi-coke, from which it could be possible to create valuable porous materials with high surface areas. These adsorbents could be used in a wide range of environmental and industrial applications. To produce adsorbents, it is first important to characterise the source material and to find out to what extent the surface area differs depending on the particle size. Considering the above, seventeen oil shale fractions, with particle sizes ranging from 36  $\mu\text{m}$  to 8 mm, were characterised in terms of total organic carbon (TOC) content, specific surface area (SSA) and porosity. Special attention was paid to the analysis of SSA using Brunauer-Emmett-Teller (BET) theory. The SSA of the studied oil shale was found to vary from 4 to 13  $\text{m}^2/\text{g}$  depending on the particle size. The analyses performed supported the known trend that the finer fractions have slightly higher contents of organic matter (i.e. kerogen) as well as higher surface areas. In addition, preliminary pyrolysis tests with the oil shale fractions were also carried out to see the effect of thermal treatment on surface area. After treatment, BET surface areas were in the range of 19–38  $\text{m}^2/\text{g}$ . As the final goal is to obtain activated carbon with a large SSA, it is important to know if and how much the results are affected by the source material. The present study provides fundamental knowledge about the source material that will enable applied research in the future.

### 1. Introduction

Oil shale is a sedimentary rock consisting of mineral and organic matter (i.e. kerogen) (Foltin et al., 2017). Kerogen can be converted into oil, gas and semi-coke by thermal degradation (Ma and Li, 2018). Shale oil is a liquid fuel produced from oil shale and obtained by thermal decomposition of the organic part of oil shale and condensation of oil vapours.

In 2018, 16 M t of oil shale was mined in Estonia. Today, Estonia is one of the largest producers of shale oil in the world – 1.1 M t of shale oil was produced in 2018 (Maaten et al., 2020). It can be calculated that for producing one ton of shale oil, approximately four t of semi-coke waste is inevitably generated (Gusca et al., 2015). Currently, semi-coke is predominantly going to waste, namely deposited in landfills (Pihu et al., 2019). However, oil shale semi-cokes could be used after pre-treatment potentially as adsorbents, which could be applied in separation, purification, and recovery processes. Preparation of an adsorbent generally involves conversion of the organic material, which is achieved by thermal treatment. As mentioned above, thermal treatment (in particular pyrolysis) is already used for shale oil production (Neshumayev et al., 2019). This makes the idea of this study also very practical as the by-product semi-coke could be effectively used. For producing a porous adsorbent material, the specific surface area (SSA) and porosity of the product are two of the main parameters related to material adsorption efficiency. Generally, the higher the SSA and more evolved porosity, the better the adsorbent.

In fact, the sorptive potential of oil shale semi-coke has been investigated before. In this regard, Külaots et al. (2010) analysed oil shale samples from Estonia, China and the United States. Authors pyrolysed samples at 500 and 1,000  $^{\circ}\text{C}$  and analysed the products for organic char content, surface area and porosity. Pyrolysis of the oil shales at 500 and 1,000  $^{\circ}\text{C}$  yielded semi-cokes with BET surface areas of 4.4–57  $\text{m}^2/\text{g}$ . Bai et al. (2012) studied experimentally the effects of pyrolysis temperature (350–450  $^{\circ}\text{C}$ ) and heating rate (2.5 to 20  $^{\circ}\text{C}/\text{min}$ ) on

the pore structure of Huadian oil shale. By varying these conditions, BET surface areas changed from 4.5 to 48.1 m<sup>2</sup>/g. They found that a slower heating rate favours the development of pores and that in the temperature range of 400–550 °C the SSA and total pore volume increase to great extent. They also pointed out that N<sub>2</sub> adsorption/desorption isotherms of oil shale and semi-coke samples can be categorised as Type II isotherms according to the IUPAC classification system.

In addition, several applications of adsorbents from oil shale have also been investigated. In this regard, Khouya et al. (2004) prepared activated adsorbents from Moroccan oil shales to eliminate U, Th, Ra, Ac and Tl from aqueous solutions. The adsorbents were produced by the pyrolysis of the oil shale at 550 °C, which was followed by KMnO<sub>4</sub> activation. No information about the SSA of the obtained product was provided in the article. Elhammoudi et al. (2017) also prepared activated carbon based on Moroccan oil shale. They concentrated oil shale with hydrochloric acid and later activated it with sulphuric acid followed by thermal treatment. They used scanning electron microscope (SEM) and Fourier-transform infrared spectroscopy (FTIR) analysis to confirm the adsorption performance of activated carbon from oil shale. The maximum adsorption capacity of cadmium was determined to be 55.87 mg/g. Nassef and Eltaweel (2019) investigated Egyptian oil shale as a source for producing an adsorbent for removal of zinc from aqueous solutions. They found that thermally or chemically activated oil shale can successfully remove high amount of Zn<sup>2+</sup> ions from an aqueous solution (up to 99%). Ermagambet et al. (2018) used Kendyryk shale to produce a porous carbon material (activated shale). For this purpose, they thermally treated the shale at temperatures of 700–800 °C in argon and activated with water vapour. After such treatment, the SSA increased from 15.6 to 131.7 m<sup>2</sup>/g. The resulting activated shale was successfully tested as an adsorbent to purify a wastewater sample.

The present study focused on locally available oil shale for which a high availability and low cost leads to its consideration as a suitable source to produce adsorbent materials. To the authors' knowledge, there has been no systematic study about the properties (surface area, porosity) of an oil shale depending on the particle size. The aim of this work was to characterise different fractions of oil shale to find out differences among them. In addition, pyrolysis of different fractions was also carried out to see the effect of thermal treatment on the surface area.

## 2. Experimental

### 2.1 Materials and methods

The oil shale sample was obtained from the Ojamaa mine, Estonia. The oil shale sample was crushed and divided into 17 fractions using a Fritsch Analysette 3 PRO vibratory sieve shaker.

Analysis of the specific surface area (SSA) and porosity was performed using an automated Quantachrome Autosorb iQ-C instrument. For the surface area analysis, approximately 0.5–1 g of oil shale was placed into a sample vial and degassed at 140 °C for 24 h. The isotherms of oil shale fractions were obtained by recording altogether eighty nitrogen adsorption and desorption data points at relative pressures ( $P/P_0$ ) from 0.025–0.995. The adsorption data points were used to calculate the BET surface areas and the porosities of each of the oil shale fractions. The pore-size distributions of oil shale were determined from the nitrogen adsorption isotherms at -196 °C using density functional theory (DFT). Elemental analysis for evaluating total organic carbon (TOC) content was performed on a Vario MACRO CHNS analyser.

Pyrolysis experiments were carried out using a tube furnace consisting of a gas dosing system, a temperature-controlled oven and a controlled gas cooling chamber capable of producing a laboratory quantity of semi-coke. For pyrolysis experiments, approximately 1 g of each oil shale fraction was placed into a porcelain crucible, which was inserted into a tube furnace maintained at one of two temperatures, 600 or 900 °C, for 30 min under a nitrogen flow of 200 mL/min. For the surface area analysis of the obtained semi-cokes, approximately 0.5 g of the sample was placed into a sample vial and degassed at 300 °C for 24 h. For the oil shale semi-coke samples, only the BET surface areas were determined.

Zeiss EVO/MA15 Scanning Electron Microscope was used for imaging oil shale and semi-coke samples.

## 3. Results and discussion

### 3.1 Surface area and porosity characterisation of oil shale fractions

Isotherms are different for each substance, and a lot of information can be derived from them. Figure 1 presents the N<sub>2</sub> adsorption and desorption isotherms of the Estonian oil shale, where four different fractions are shown for comparison: 36–45 μm, 500–710 μm, 1.4–2.0 mm and 5.6–8.0 mm. The oil shale fractions studied can be categorised as Type II isotherms according to the IUPAC classification system, which are characteristic to materials that are either macroporous or not very porous. Other researchers (Bai et al., 2012) have obtained similar results. Comparing these isotherms, it can be seen that the shapes of these isotherms as a whole are

somewhat similar, and different fractions have a similar microporosity. However, it is noticeable that the adsorption capacity for finer fractions is higher than that of bigger particles.

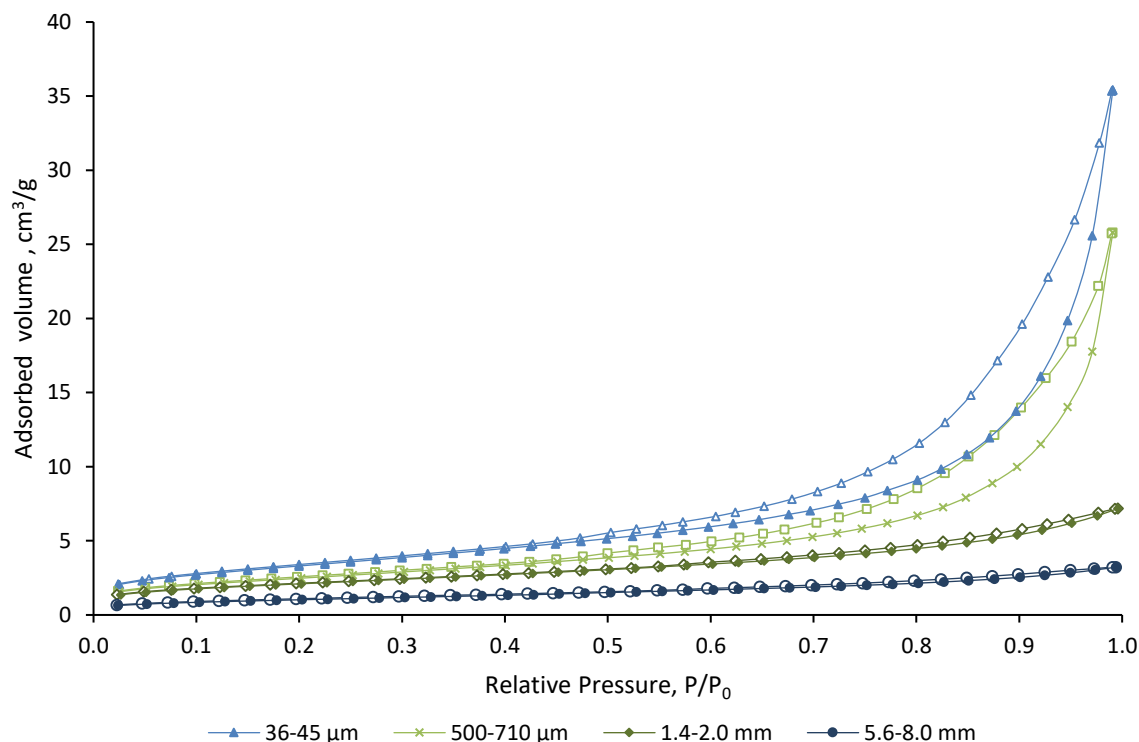


Figure 1:  $N_2$  adsorption and desorption isotherms of four Estonian oil shale fractions: 36-45  $\mu\text{m}$ , 500-710  $\mu\text{m}$ , 1.4-2.0 mm and 5.6-8.0 mm. Filled markers: adsorption, unfilled markers: desorption branches

The adsorption branches of the isotherms of smaller fractions (36-45 and 500-710  $\mu\text{m}$ ) rise slowly up to a relative pressure of 0.8 and then rise more sharply. The rise of branches of bigger particles (1.4-2.0 mm and 5.6-8.0 mm) is modest (as expected). It can be seen from Figure 1 that the desorption branches of finer fractions do not coincide with the corresponding adsorption branches and form hysteresis loops. The appearance of hysteresis is usually associated with capillary condensation in mesopore structures (Sing et al., 1985). According to the IUPAC classification system, hysteresis loops are divided into four types and some information about the pore structure can be derived from the type of hysteresis loop. In this study, the hysteresis of the oil shale samples is similar to the H3 type hysteresis loop, which refers to slit-shaped pores. The H3 type is also associated with absence of micropores, or very few of them (since there is a small uptake in low  $P/P_0$  range). For the H3 type, BET theory can be applied in the common  $P/P_0$  range (0.05 - 0.3). In this work, seven adsorption data points of relative pressures from 0.1 to 0.3 were used to calculate the BET surface areas. The results are presented in Table 1. The BET surface areas of all oil shale fractions ranged from 3.8 to 12.6  $\text{m}^2/\text{g}$ . As expected, the smaller the particle size, the bigger the surface area. The SSA increased three times from particle size of 8.0 mm to 36  $\mu\text{m}$ , whereas SSA remained more or less the same in the diameter range of 36-125  $\mu\text{m}$  ( $12.3 \pm 0.2 \text{ m}^2/\text{g}$ ). Total pore volume is calculated from the amount of the gas adsorbed at a relative temperature close to unity ( $P/P_0 = 0.99$  in this case) and the average pore size is estimated from the total pore volume. Total pore volumes are given for each fraction in Table 1, which shows a clear increase with decreasing particle size. Average pore diameters of the oil shale samples were calculated to be in the range of 5-18 nm. The average pore diameter in fractions with a particle size from 1.4 to 8 mm was 5 nm, while for fractions less than 1 mm it was 17 nm. That indicates that the higher SSA is due to the appearance of mesopores in finer fractions.

The pore size distribution determines the applicability of the material for different uses. Typically, adsorbents with high surface areas and porosities are preferred. As written before, H3 type hysteresis loop refers to slit-shaped pores and the suitable calculation method for pore size distribution analysis is DFT (Schindler et al., 2013).

Table 1: BET surface areas, total pore volumes and TOC contents of the oil shale; BET surface areas of the obtained semi-cookes after oil shale pyrolysis at 600 or 900 °C in nitrogen

Fraction size	BET surface area of oil shale, m <sup>2</sup> /g (n = 3, RSD < 3 %)	Total pore volume at P/P <sub>0</sub> =0.99, cm <sup>3</sup> /g (n = 3, RSD < 3 %)	TOC, % (n = 3, RSD < 3 %)	BET surface area of semi-coke (600 °C), m <sup>2</sup> /g (n = 3, RSD < 6 %)	BET surface area of semi-coke (900 °C), m <sup>2</sup> /g (n = 3, RSD < 4 %)
5.6–8.0 mm	3.8	0.005	26.2	25.8	26.0
4.0–5.6 mm	5.8	0.008	21.4	n.d.	n.d.
3.15–4 mm	6.1	0.026	18.4	20.0	19.7
2.8–3.15 mm	8.0	0.015	20.2	n.d.	n.d.
2.0–2.8 mm	7.7	0.013	21.9	20.8	24.8
1.4–2.0 mm	7.5	0.011	21.6	n.d.	n.d.
1.0–1.4 mm	8.3	0.033	20.4	18.8	25.6
710–1,000 μm	8.9	0.037	20.5	n.d.	n.d.
500–710 μm	9.2	0.040	19.7	19.6	30.4
355–500 μm	10.2	0.044	20.2	n.d.	n.d.
250–355 μm	10.4	0.044	20.9	19.9	18.9
180–250 μm	11.5	0.050	23.3	n.d.	n.d.
125–180 μm	12.3	0.053	26.3	29.0	27.0
90–125 μm	12.6	0.052	29.1	n.d.	n.d.
63–90 μm	12.4	0.054	30.6	37.6	31.6
45–63 μm	12.0	0.054	31.3	n.d.	n.d.
36–45 μm	12.3	0.055	31.1	35.7	29.9

RSD – relative standard deviation, n.d. – not determined

Figure 2 shows the results of DFT pore-size distribution analysis of Estonian oil shale. Figure 2 clearly illustrates that finer fractions have more mesopores (diameter 2-50 nm according to IUPAC), while the microporosity of all fractions is similar (pores smaller than 2 nm in diameter).

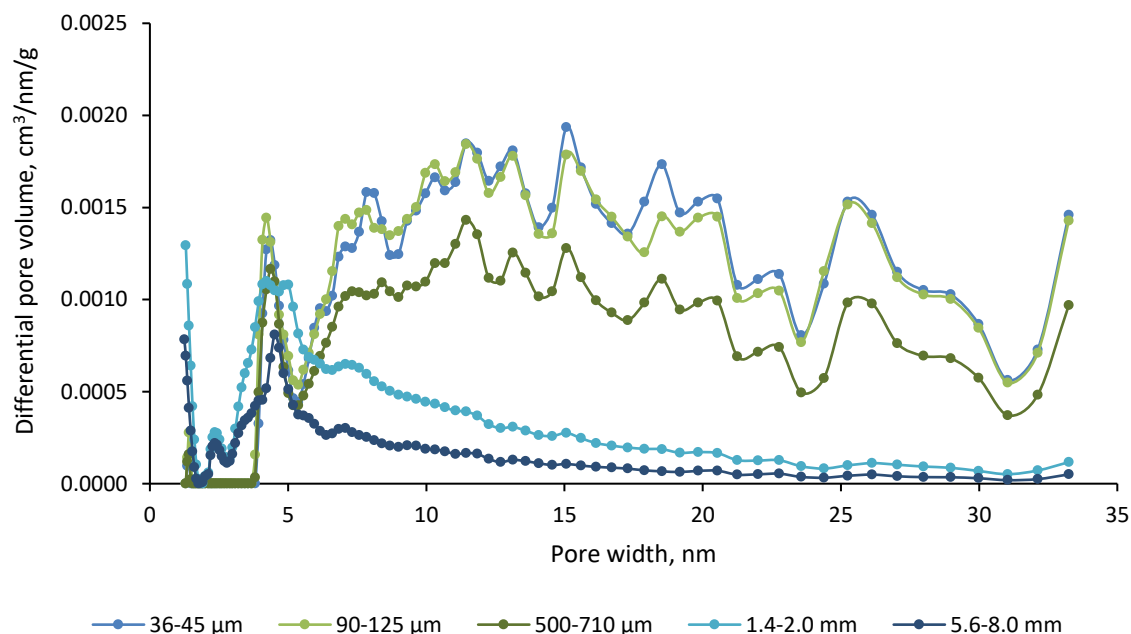


Figure 2: DFT pore-size distribution of five oil shale fractions

It is not surprising that the SSA is dependent on the particle size. However, as there are previously published results about correlations between TOC content and SSA, this was of interest for the present work, too (Cao et al., 2015). The results in Table 1 show that generally particles with smaller diameters have higher TOC contents. The TOC content varied from 18.4 to 31.3 % with the highest content in the fractions with the smallest particle

sizes (36-90  $\mu\text{m}$ ). However, in this work poor correlation was found between SSA and TOC content ( $R^2=0.63$  for a linear fit) of Estonian oil shale. Better correlation was obtained if only smaller particles (36-500  $\mu\text{m}$ ) were taken into account:  $R^2=0.8$  for a linear fit. This result is in accordance with the previously published article by Cao et al. (2015), where poor correlation was also found between SSA and the TOC content of the Permian Dalong Formation shales.

### 3.2 Semi-coke samples after thermal treatment of the oil shale

In order to see the effect of thermal treatment on SSA, preliminary pyrolysis tests of nine oil shale fractions were carried out. Oil shale samples were pyrolysed for 30 min at 600 and 900  $^{\circ}\text{C}$  in nitrogen and the BET surface areas of the products were determined. After such thermal treatment, the BET surface areas of nine oil shale fractions ranged from 19 to 38  $\text{m}^2/\text{g}$  (Table 1). The highest surface areas were obtained with finest fractions (36-90  $\mu\text{m}$ ) after thermal treatment at 600  $^{\circ}\text{C}$ , being  $36.7 \pm 1.4 \text{ m}^2/\text{g}$ . Generally, the surface areas increased up to 2–3 times after thermal treatment of the oil shale. As an exception, the biggest particles, i.e. > 5.6 mm, exhibited a larger change in SSA due to the fact that bigger particles were prone to break during thermal treatment.

Some interesting tendencies can be seen from the results. Firstly, there was no big difference in SSA with bigger particles (>3.15 mm) no matter the treatment temperature. Secondly, with particles from 500  $\mu\text{m}$  to 3.15 mm higher surface areas were obtained with treatment at higher temperature (900  $^{\circ}\text{C}$ ), while with particles below that size (36–500  $\mu\text{m}$ ) the SSA started to decrease with higher temperature. For example, with 500-710  $\mu\text{m}$  particles, the SSA increased from 20 to 30  $\text{m}^2/\text{g}$  comparing temperatures 600 and 900  $^{\circ}\text{C}$ , while with 36-45  $\mu\text{m}$  particles the reversed effect was noticed – a decrease from 36 to 30  $\text{m}^2/\text{g}$  at temperatures of 600 and 900  $^{\circ}\text{C}$ . The reason for this might lie in the different heat transfer of the particles – finer fractions are more exposed to heat than bigger particles, and, at some temperature, the structure can start to collapse resulting in a smaller SSA. In fact, Ouyang et al. (2013) obtained similar results with anthracite powder. They found that heating temperature can be divided into two regions: below 900  $^{\circ}\text{C}$  and above 900  $^{\circ}\text{C}$ . Below 900  $^{\circ}\text{C}$ , the SSA and pore volume increased rapidly due to the quick heating of particles; while above 900  $^{\circ}\text{C}$ , the SSA and pore volume decreased as the result of the pore collapse and coal softening.

Generally, after treatment at 600  $^{\circ}\text{C}$ , no big difference in SSAs was observed between particles for 250  $\mu\text{m}$  to 4 mm, with the SSA being  $19.8 \pm 0.7 \text{ m}^2/\text{g}$ . After oil shale treatment at 900  $^{\circ}\text{C}$ , SSA varied over the studied particle range from  $26.0 \pm 4.5 \text{ m}^2/\text{g}$ . With both temperatures, the highest surface areas were obtained with the finest fractions.

Results demonstrate that even using a simple thermal treatment process a carbonised material with a considerable BET area was obtained – overall surface area varied in the range of 19 to 38  $\text{m}^2/\text{g}$  (Table 1). These results are in accordance with the previously published results by Kõlaots et al. (2010), where it was outlined that the BET surface areas for different oil shale semi-cokes were between 4–57  $\text{m}^2/\text{g}$ . For better visualisation, SEM images of raw material and pyrolysis products are depicted in Figure 3. The appearance of pores after pyrolysis is even visually clear. In Figure 3A, an oil shale sample with particle size between 500 to 710  $\mu\text{m}$  is shown (SSA around 9  $\text{m}^2/\text{g}$ ). In Figure 3B and 3C, oil shale samples with the same particle size after pyrolysis in nitrogen at 600  $^{\circ}\text{C}$  (B) and 900  $^{\circ}\text{C}$  (C) are shown – SSAs approximately 20 and 30  $\text{m}^2/\text{g}$ . It can be seen from Figure 3 that in the raw material most of the pores are closed while after thermal treatment pore mouths have opened.

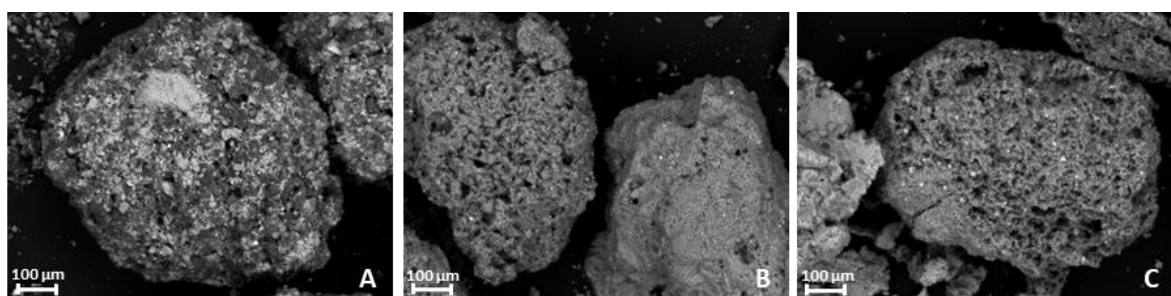


Figure 3: SEM images of oil shale (A) and semi-coke (B,C) samples. In all images, particle size 500-710  $\mu\text{m}$  and magnification 300x. Thermal treatment of oil shale carried out at 600  $^{\circ}\text{C}$  (B) and 900  $^{\circ}\text{C}$  (C) in nitrogen

## 4. Conclusions

Aim of this article was to investigate oil shale as a raw material to produce porous materials, i.e. adsorbents. The idea of the present study is very practical as thermal treatment is already used for shale oil production and semi-coke is concurrently generated as a by-product. The use of the latter as an adsorbent material would optimise the shale oil production process and reduce pollution. To the authors' best knowledge, there has been

no systematic study about the surface area of an oil shale depending on the particle size. Yet, surface area is one of the key factors defining the usability of an adsorbent. For that purpose, different size of oil shale particles were studied to see the difference and change in the BET surface area. The results with the raw material indicated that over the range of particle size from 36  $\mu\text{m}$  to 8.0 mm the change in the surface area was 3-fold: from 4 to 12  $\text{m}^2/\text{g}$ . The surface areas of particles from 36-125  $\mu\text{m}$  were similar, being  $12.3 \pm 0.2 \text{ m}^2/\text{g}$ . As the ultimate goal in the future would be to produce porous materials from oil shale, simple pretreatment of the raw material was performed. For that purpose, the studied oil shale fractions were pyrolysed for 30 min at 600 and 900  $^{\circ}\text{C}$  in nitrogen. After such treatment, the surface area of the obtained semi-coke was up to 2-3 times higher than that of the raw material and was in the range of 19 to 38  $\text{m}^2/\text{g}$ . The highest SSAs were obtained with the finest fractions when pyrolysed at 600  $^{\circ}\text{C}$ . It was also observed that SSAs of finer fractions started slightly to decrease at 900  $^{\circ}\text{C}$ . The authors believe that these are quite promising results for the future since chemical and physical activation has not even been applied yet, which would increase the SSA even more.

### Acknowledgements

This work was supported by the Estonian Research Council grant (PSG266).

### References

- Bai J., Wang Q., Jiao G., 2012, Study on the pore structure of oil shale during low-temperature pyrolysis, *Energy Procedia*, 17, 1689–1696.
- Cao T., Song Z., Wang S., Xia J., 2015, A comparative study of the specific surface area and pore structure of different shales and their kerogens, *Science China: Earth Sciences*, 58, 510–522.
- Elhammoudi N., Oumam M., Mansouri S., Chham A., Abourriche A., Hannache H., 2017, Preparation and development of a novel activated carbon based on moroccan oil shale using activation process, *American Journal of Chemistry*, 7, 163–170.
- Ermagambet B.T., Kasenov B.K., Nurgaliyev N.U., Kazankapova M.K., Kasenova Z.M., Zikirina A.M., 2018, Adsorbent Production using oil shale from the kendyrlyk deposit, *Solid Fuel Chemistry*, 52, 302–307.
- Foltin J.P., Prado G.N., Lisboa A.C.L., 2017, Analysis of kinetics parameters of oil shale pyrolysis, *Chemical Engineering Transactions*, 61, 439–444.
- Gusca J., Siirde A., Eldermann M., 2015, Energy related sustainability analysis of shale oil retorting technologies, *Energy Procedia*, 72, 216–221.
- Khouya E., Fakhi S., Hannache H., Abbe J.C., Andres Y., Naslain R., Pailler R., Nouredine A., 2004, New adsorbents from oil shales: Preparation, characterization and U, Th isotope adsorption tests, *Journal of Radioanalytical and Nuclear Chemistry*, 260, 159–166.
- Külaots I., Goldfarb J.L., Suuberg E.M., 2010, Characterization of Chinese, American and Estonian oil shale semicokes and their sorptive potential, *Fuel*, 89, 3300–3306.
- Ma Y., Li S., 2018, The mechanism and kinetics of oil shale pyrolysis in the presence of water, *Carbon Resources Conversion*, 1, 160–164.
- Maaten B., Järvik O., Pihl O., Konist A., Siirde A., 2020, Oil shale pyrolysis products and the fate of sulfur, *Oil Shale*, 37, 51–69.
- Nassef E., Eltaweel Y., 2019, Removal of Zinc from aqueous solution using activated oil shale, *Journal of Chemistry*, 2019, 1–9.
- Neshumayev D., Pihu T., Siirde A., Järvik O., Konist A., 2019, Solid heat carrier oil shale retorting technology with integrated CFB technology, *Oil Shale*, 36, 99–113.
- Ouyang Z., Zhu J., Lv Q., Wang J., Hou H., 2013, Particle characteristics of anthracite powder preheated quickly in circulating fluidized bed, 2013 International Conference on Materials for Renewable Energy and Environment, Chengdu, China, 796–801.
- Pihu T., Konist A., Puura E., Liira M., Kirsimäe K., 2019, Properties and environmental impact of oil shale ash landfills, *Oil Shale*, 36, 257–270.
- Schindler B.J., Mitchell L.A., McCabe C., Cummings P.T., LeVan M.D., 2013, Adsorption of chain molecules in slit-shaped pores: Development of a SAFT-FMT-DFT approach, *The Journal of Physical Chemistry C*, 117, 21337–21350.
- Sing K.S.W., Everett D.H., Haul R.A.W., Moscou L., Pierotti R.A., Rouquerol J., Siemieniewska T., 1985, Reporting Physisorption Data for Gas/Solid Systems with Special Reference to the Determination of Surface Area and Porosity, *Pure and Applied Chemistry*, 57, 603–619.